A Variational Model for Interactive Shape Prior Segmentation and Real-Time Tracking

Manuel Werlberger, Thomas Pock, Markus Unger, and Horst Bischof

Institute for Computer Graphics and Vision, Graz University of Technology
{werlberger,pock,unger,bischof}@icg.tugraz.at
http://www.gpu4vision.org

Abstract. In this paper, we introduce a semi-automated segmentation method based on minimizing the Geodesic Active Contour energy incorporating a shape prior. We increase the robustness of the segmentation result using the additional shape information that represents the desired structure. Furthermore the user has the possibility to take corrective actions during the segmentation and adapt the shape prior position. Interaction is often desirable when processing difficult data like in medical applications. To facilitate the user interaction we add a shape deformation which allows to change the shape position manually by the user and automatically in terms of underlying image features. Using a variational formulation, the optimization can be done in a globally optimal manner for a fixed shape representation. To obtain real-time behavior, which is especially important for an interactive tool, the whole method is implemented on the GPU. Experiments are done on medical, as well as on video data and camera streams that are processed in real-time. In terms of medical data we compare our method with a segmentation done by an expert. The GPU based binaries will be available online on our homepage.

1 Introduction

Image segmentation is a very common problem in computer vision. Many segmentation methods use low-level features to obtain a division into fore- and background. Due to the need of robustness it has become a common practice to incorporate high level knowledge to gain reasonable results. The method presented in this paper enhances the robustness of segmentation by imposing shape information of the desired object which allows a precise result with difficult image data (Fig. 1). Pioneering contributions have been made by Cremers et al. [1] with their variational approach of 'Diffusion Snakes', the level set formulation by Leventon et al. [2, 3] as well as the region based approach by Paragios and Rousson [4, 5].

The efficient registration of the shape prior to the desired image structure is a challenging problem. Therefore we developed a semi-automated segmentation tool that allows to adjust the object position by hand and by a local optimization routine which is modelled as shape transformation in either case. For the

X.-C. Tai et al. (Eds.): SSVM 2009, LNCS 5567, pp. 200–211, 2009.

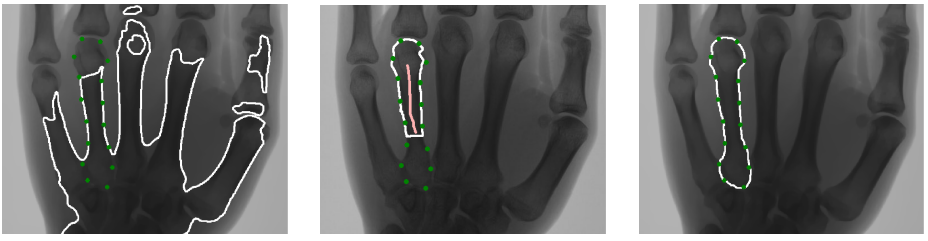

Fig. 1. Segmentation of the metacarpal bone of a ring finger. The **left image** shows a simple intensity thresholding which clearly fails. The pure GAC segmentation in the **middle image** does not result into a valid segmentation either. The shape prior segmentation in the **right image** can also deal with the low-contrast regions and provides an accurate result.

realization of the segmentation method we use a variational formulation of the Geodesic Active Contour (GAC) energy. The minimization is done with a fast primal-dual approach that is implemented using NVIDIA graphics hardware to become real-time capable. Therefore the method can even be used for tracking objects in videos or live camera streams. Approaches based on the calculus of variation have had great success and recently it has been shown that variational methods show good parallelization capabilities that benefit from a GPU implementation [6, 7].

The main contribution of our work is the incorporation of a shape representation into a variational segmentation framework. We show that the resultant segmentation is globally optimal for a fixed shape prior and provide a GPU implementation for a fast primal-dual optimization procedure defining a definite convergence criterion. Therefore we can add the possibility to interact with the shape position and get a segmentation result in real-time. The framework permits a local optimization of the shape position to get a correct segmentation of objects with a preceding misalignment of the prior.

The remainder of the paper is organized as follows: First we give an overview of related work. Section 3 discusses the method on combining a shape prior with a variational formulation of the GAC segmentation model which leads to a segmentation model utilizing a Mumford-Shah (MS) like data term as shape force. In Section 3.1 we propose a fast numerical algorithm to compute the solution of the segmentation model. In 4 we present experiments and a qualitative assessment on reference data. Finally, Section 5 gives a short conclusion.

2 Related Work

2.1 Mumford-Shah Segmentation

In [8], Mumford and Shah (MS) proposed a segmentation model of the form

$$\min_{u,\Gamma}\Big\{\int_{\Omega}(u-f)^2\;dx+\alpha\int_{\Omega\setminus\Gamma}|\nabla u|^2\;dx+\beta\,\mathrm{length}\,(\Gamma)\Big\} \tag{1}$$

where f denotes the observed image, u its piecewise smooth approximation and Γ represents the edges in u. Equation (1) is based on a piecewise smooth approximation of the intensity function and was used in the computer vision community for various tasks like denoising, inpainting, stereo matching, segmentation and many more. A special case of the MS model to segment an image into fore- and background was proposed with the so-called piecewise constant MS segmentation model (2) that was later used by Chan and Vese [9] in combination with a level-set optimization.

$$\min_{\Sigma, c_1, c_2} \left\{ \mathrm{Per}\,(\Sigma) + \lambda \int_{\Sigma} (f - c_1)^2 \, dx + \lambda \int_{\Omega \setminus \Sigma} (f - c_2)^2 \, dx \right\} \tag{2}$$

In (2) f denotes the input image and c_1, c_2 the mean values of the fore- and background intensities separated by the region Σ. This realization of the MS functional represents the Potts model [10] for two distinct classes. In addition Chan et al. provided a convex formulation in [11] in form of a Total Variation (TV) functional for a binary segmentation $u = \mathbf{1}_{\Sigma}$:

$$\min_{u \in \{0,1\}} \left\{ \int_{\Omega} |\nabla u| \, dx + \lambda \int_{\Omega} u s\,(x) \, dx \right\} \tag{3}$$

with

$$s\,(x) = (c_1 - f\,(x)\,)^2 + (1 - u)\,(c_2 - f\,(x)\,)^2 \tag{4}$$

and with $\int_{\Omega} |\nabla u| \, dx$ being the TV-norm in a distributional sense $\int_{\Omega} |D\,u|$. Due to the fact that we are working on image data which can be interpreted as sufficient smooth functions, the TV-norm is valid for any input u and we stick to the notation $\int_{\Omega} |\nabla u| \, dx$ in this paper. For this formulation the TV-norm denotes the length of the segmentation: $\int_{\Omega} |\nabla u| \, dx = \mathrm{Per}\,(\Sigma)$.

Moreover Chan et al. [11] showed that a global minimizer can be found for (2) with a restricted minimization of the relaxed problem (3) so that $0 \leq u \leq 1$. The minimization set is then given by

$$\Sigma = \left\{ x \in \Omega : u > \mu \right\}, \quad \text{for every } \mu \in (0, 1)\,. \tag{5}$$

2.2 Geodesic Active Contours

Based on the Snake model of Kass et al. [12], Caselles et al. [13] and Kichenassamy et al. [14, 15] proposed an energy that is invariant with respect to new parametrizations of the contour. The Geodesic Active Contour (GAC) (in 3D the model is called minimal surface) is defined as the variational problem

$$\min_{C} \left\{ \int_0^{|C|} g\,(|\nabla I\,(C(s))|)\, ds \right\}, \tag{6}$$

where $|C|$ describes the Euclidean length of the curve C and the function g models an edge detector. The edge strength has to be restricted to an interval $g \in (0, 1]$. One common choice for computing g is

$$g(|\nabla I|) = e^{-\eta |\nabla I|^{\kappa}}, \qquad \text{for some reasonable parameters } \kappa \text{ and } \eta. \tag{7}$$

The general intention of the Snake model is to locate the curve at points with a high edge strength and keep a certain smoothness in the curve. The main advance of GACs is the profound mathematical framework that makes the model very versatile for different applications. The main drawbacks of the model are the non-convexity of the GAC energy and that the empty set is always a global minimizer of (6).

In [16, 17, 18], several authors proposed the so-called weighted Total Variation (8) that can be used to give an alternative formulation of the GAC energy. They showed that if $u = \mathbf{1}_{\Omega_C}$ is a binary function with C the boundary of Ω_C, the energy (8) equals the GAC energy (6).

$$TV_g(u) = \int_\Omega g\,|\nabla u|\;dx \tag{8}$$

Note that the weighted TV-norm is similar to the regularization term of (3). The additional weighting function g is a pointwise constant multiplier and therefore the method of Chan et al. [11, 19] mentioned in the previous Section 2.1 is still valid. Based on these assumptions they showed that by replacing $\mathbf{1}_{\Omega_C}$ with $u \in [0, 1]$, (8) becomes convex, allowing to compute a global minimizer. However, there remains the problem that the empty set depicts a global optimal solution. In [6, 7], Unger et al. proposed a variational formulation incorporating user constraints that avoid this drawback of the classical GAC model.

3 Shape Prior Segmentation

Our main contribution is to combine GAC segmentation and a MS-like data term to incorporate shape information. Therefore we model the GAC energy with the weighted Total Variation (8) and utilize the need of additional constraints by imposing the shape prior.

Starting with a formulation of the Mumford-Shah like energy utilized by Chan and Vese in [9] we obtain a variational optimization problem like in (3). The multiplicative part in the data-term will be used as shape information $s\,(x)$ to model the shape prior segmentation energy. In addition we use the weighted Total Variation (8) to model the GAC energy and add a parameter λ to balance between regularization and shape force:

$$\min_{0\le u\le 1}\Big\{\int_\Omega g\,|\nabla u|\;dx + \lambda\int_\Omega s\,(x)\,u\,dx\Big\} \tag{9}$$

For a low λ the result of the GAC will be preferred, whereas for increasing λ the shape prior will be taken more into account. In Fig. 2 the effects of different parameter settings are shown. Since (9) is homogeneous of degree one, the thresholding theorem of [11] still applies in our case, allowing us to compute the global minimizer of (9) as mentioned in Section 2.1 according the MS segmentation model (3). The optimization method will be discussed in more detail in the following Section 3.1.

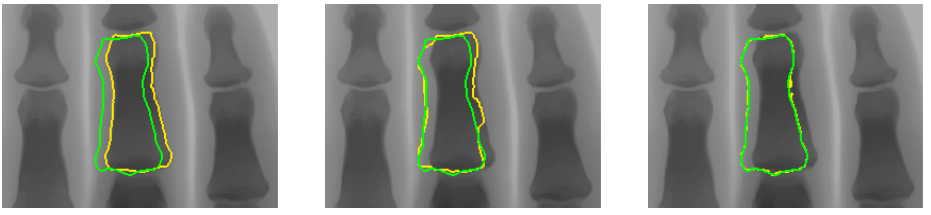

Fig. 2. Evaluation of different settings of λ: The images show that with increasing $\lambda = \{0.01,\ 0.02,\ 0.1\}$ (left to right) the segmentation is more attracted to the fixed shape. For a low λ the influence of the pure GAC energy increases and the segmentation is more attracted to significant edges.

The shape prior itself influences the segmentation by setting pixelwise fore- and background constraints which are modelled in the following way:

$$\begin{aligned} s\,(x) &< 0 \quad \ldots \quad \text{Foreground} \\ s\,(x) &> 0 \quad \ldots \quad \text{Background} \end{aligned} \tag{10}$$

Therefore one can use different types of shape representations. As a simple example we defined the shape $s\,(x)$ as a binary function with $s\,(x) = -1$ within the shape region and $s\,(x) = 1$ outside similar to [20] where Cremers et al. use subspace methods to learn a representative set of shapes. Binary functions are used to encode shapes which lead to problems when interpolating between two instances. As a consequential step we use a signed-distance map with the constraints (10) which implicitly includes a distance information towards the shape boundary. That means for our algorithm that the more a pixel is within the shape boundary, the more likely this region belongs to the desired segmentation. In Fig. 5 we show the benefit on using a signed-distance map as shape representation compared to a binary one. This representation and the combination with a GAC energy allows to handle deformations with a single prior.

3.1 Solving the Shape Prior Segmentation Model

It is well known that functionals like (9) are difficult to optimize due to the L^1-norm $|\nabla u|$. Chan et al. [21], Carter [22] and Chambolle [23, 24] proposed a dual formulation for optimizing the classical variational problem of Rudin, Osher and Fatemi [25] for image denoising. Such a primal-dual approach can be applied to our minimization problem (9). The main intention is to remove the singularity by introducing the dual formulation of the weighted TV-norm

$$\int_\Omega g\,|\nabla u|\ dx = \max_{||\boldsymbol{p}||\leq g} \Big\{ - \int_\Omega u\ \mathrm{div}\,\boldsymbol{p}\ dx \Big\}, \tag{11}$$

where $\boldsymbol{p} = \left(p^1, \ldots, p^d\right)^T : \Omega \to \mathbb{R}^d$ is the dual variable with d being the problems dimension. Combining this maximization problem with the initial minimization task (9) this leads to

$$\min_{0\leq u\leq 1}\max_{||\boldsymbol{p}||\leq g}\Big\{-\int_\Omega u\ \mathrm{div}\,\boldsymbol{p}\,dx+\lambda\int_\Omega s\,(x)\,u\,dx\Big\}. \tag{12}$$

For a fixed shape prior the outline of the primal-dual optimization algorithm is given as follows:

1. **Primal update:** The primal update accomplishes the segmentation update and therefore performs the optimization according to the minimization of u:

$$\frac{\partial}{\partial u}\Big\{-\int_\Omega u\cdot\ \mathrm{div}\,\boldsymbol{p}\,dx+\lambda\int_\Omega s\,(x)\,u\,dx\Big\}=-\,\mathrm{div}\,\boldsymbol{p}+\lambda s\,(x) \tag{13}$$

Performing a gradient descent update scheme this leads to

$$u^{n+1}=\Pi_{[0,1]}\big(u^n-\tau_P\,(-\,\mathrm{div}\,\boldsymbol{p}+\lambda s\,(x)\,)\big), \tag{14}$$

where τ_P denote the steplength and the orthogonal projection Π towards the binary set $[0,1]$ can be done with a simple thresholding step.

2. **Dual update:** The maximization according to $\boldsymbol{p}$ can be stated as

$$\frac{\partial}{\partial \boldsymbol{p}}\Big\{\int_\Omega \boldsymbol{p}\cdot\nabla u\,dx+\lambda\int_\Omega s\,(x)\,u\,dx\Big\}=\nabla u \tag{15}$$

with the additional constraint $||\boldsymbol{p}||\leq g$. This results into a gradient ascent method with a orthogonal reprojection to restrict the length of $\boldsymbol{p}$ to the weight g:

$$\boldsymbol{p}^{n+1}=\Pi_{B_0^g}\big(\boldsymbol{p}^n+\tau_D\nabla u\big) \tag{16}$$

Here B_0^g denotes a d-dimensional ball centered at the origin with the radius g. The reprojection onto B_0^g can be formulated with

$$\Pi_{B_0^g}(\mathbf{q})=\frac{\mathbf{q}}{\max\big\{1,\frac{||\mathbf{q}||}{g}\big\}} \tag{17}$$

3. **Iterate until convergence:** Solving the optimization problem (12) results in a consecutive update scheme with a gradient descent (14) and a gradient ascent step (16). Such an iterative algorithm demand on a convergence criterion. Therefore we take the energy of the single steps into account:

Primal energy: The primal energy can be calculated by solving (12) by maximizing the equation towards the dual variable $\boldsymbol{p}$. Due to (11) $\boldsymbol{p}$ can be restated as

$$\begin{aligned}\boldsymbol{p}&=\frac{\nabla u}{|\nabla u|}g \qquad \text{if } \nabla u\neq 0\\ \boldsymbol{p}&\in B_0^g \qquad \text{else}\end{aligned} \tag{18}$$

for the optimization. This results into the energy equation (19) which is the same as evaluating the energy functional (9).

$$E_{Primal}=\int_\Omega g\,|\nabla u|+\lambda\,s\,(x)\,u\,dx. \tag{19}$$

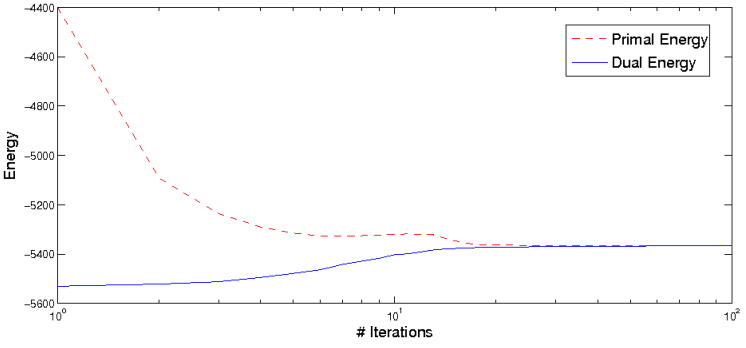

Fig. 3. Relation of primal to dual energy while optimizing with the proposed primal-dual update scheme. The plot shows the iterations in a logarithmic scale over 100 iterations. Note that after 20 iterations the primal-dual gap is small enough to stop iterating.

Dual energy: The dual energy can be formulated by minimizing (12) towards u:

$$\min_{0\leq u\leq 1}\Big\{\int_\Omega u\Big(-\operatorname{div}\boldsymbol{p}+\lambda s\left(x\right)\Big)\,dx\Big\}, \tag{20}$$

which conclude that the binary segmentation $u\in\{0,1\}$ is set to $u=1$ if the term $-\operatorname{div}\boldsymbol{p}+\lambda s\left(x\right)<0$ and $u=0$ otherwise:

$$E_{Dual}=\int_\Omega \min\Big\{-\operatorname{div}\boldsymbol{p}+\lambda s\left(x\right),0\Big\}\,dx \tag{21}$$

In [26, 27], Zhu et. al. introduce a measurement for the convergence state of primal-dual algorithms in case of the ROF model. As a criterion they use the gap between the primal and dual energy. Applied to our primal-dual optimization algorithm we get an adaption of the energies like in Fig. 3. Therefore we use a fixed stepwidth for the primal (τ_P) and dual update (τ_D) with the constraint that $\tau_P\tau_D\leq\frac{1}{2}$. For all the results shown in this paper we used $\tau_P=\tau_D=\frac{1}{\sqrt{2}}$. We also tried adaptive timesteps (τ_P,τ_D) for the optimization steps similar to the work of Zhu and Chan in [26] but did not find a reasonable equivalent for our method.

3.2 Shape Alignment

So far, our considerations assume a spatially fixed shape prior $s\left(x\right)$. In order to adapt the shape prior to different locations in the image we introduce a set of transformation parameters $\phi=\{t,R,S\}$ with the transformation parameters t for translation, R for rotation and S for the scale. Imposing this transformation into the segmentation energy (9) leads to an additional optimization parameter:

$$\min_{u,\phi}\Big\{\int_\Omega g\left|\nabla u\right|\,dx+\lambda\int_\Omega\big(\phi\left(t,R,S\right)\circ s\left(x\right)\big)u\,dx\Big\} \tag{22}$$

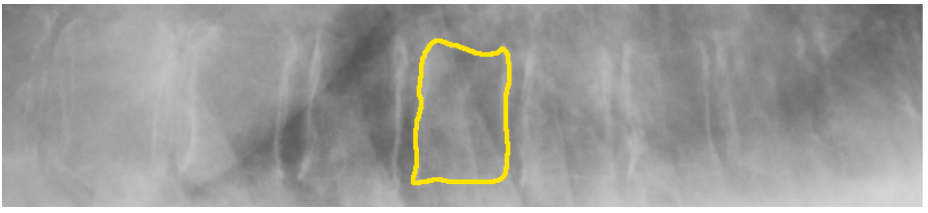

Fig. 4. Segmentation of a vertebra in an X-ray image of the spline. Due to very bad contrast the segmentation without prior would fail completely. The definition of the prior was prepared by us and therefore cannot be considered as reference data.

In [20], Cremers et al. show with the help of the Lipschitz continuity that with an integrated rigid body motion the energy functional remains convex and therefore can be optimized globally for fixed transformation parameters. They additionally show that for optimizing the shape position itself the complete subspace Ω where the energy (9) is defined has to be sampled on a rather fine grid with all possible shape positions for evaluating the minimization task in a global manner. This is of course not feasible for an interactive application due to the need of optimizing the problem in real-time. Therefore we added a semi-automated approach that allows the user to have influence on the shape position and in addition an automated search for the optimal transformation parameters in a local neighborhood can be done. The optimization scheme in Sect. 3.1 can be retained with an extension on optimizing the transformation ϕ:

1. **Solve shape prior segmentation model.**
2. **Optimize transformation parameters $\boldsymbol{\phi}$ with a fixed $\boldsymbol{u}$:** Here we use a semi-automated position optimization of the shape prior. First, the user has the possibility to do a coarse positioning of the shape and second an optimization step tries to fit the shape to desired surrounding structures. Therefore we evaluate the energy (19) for different transformations ϕ. The optimal position is found where (19) has its minimum. The user gets an immediate result while changing the shape position and therefore can directly interact with the segmentation algorithm.
3. **Iterate until convergence.**

Note that the domain of ϕ is restricted due to performance issues. Doing a complete search over the whole parameters space of the transformation parameters, a global optimal solution of (22) can be calculated like in [20].

4 Experimental Results

To reach real-time performance we have to compute the iterative solution as fast as possible. Due to the good parallelization attributes of variational algorithms we decided to implement the method using GPGPU programming with the help of NVIDIAs CUDA. The involved enhancements offer the possibility to combine

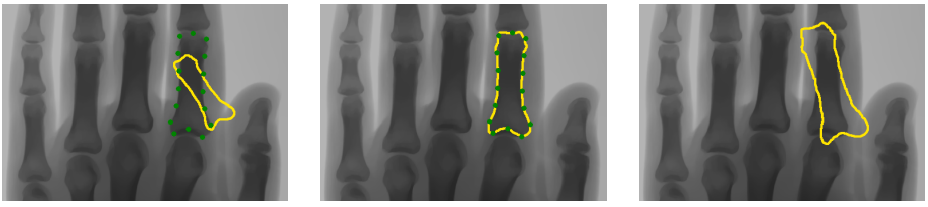

Fig. 5. The same dataset as in Fig. 1 was used to evaluate the shape alignment step. Therefore the shape prior is placed nearby the desired bone (left image) and the alignment step searches for the optimal position in the local neighborhood. The results (middle image) show that the segmentations are equivalent to the hand-labeled points. The right image shows the alignment step using a binary shape prior which fails for the optimization step. For the correct result in the middle image a signed distance representation of the shape term was used.

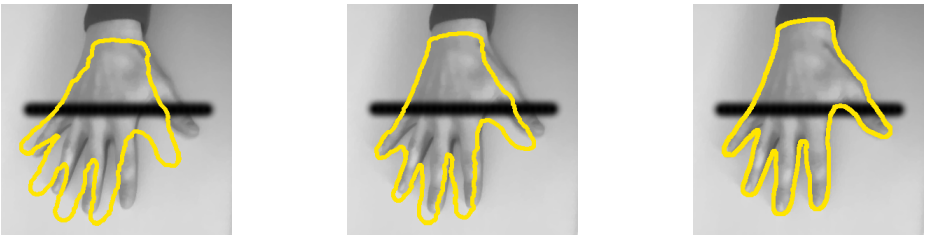

Fig. 6. The position refinement is robust against partial occlusion

user interactivity with the computational intensive variational method and get a segmentation result at interactive rates. The performance depends mainly on the size of the search region in the parameter space and on the shape prior's size as well. As an example we achieve 80 frames per second on a NVIDIA GeForce GTX 280 for pure segmentation and 20 frames per second including the position optimization.

In our Framework we have two possibilities to provide a shape prior for the segmentation. Either the user can define a shape prior directly with a segmentation of a structure using pure GAC energy by setting foreground and background seeds. This is especially useful when recurring structures have to be segmented. For more accurate results especially on difficult data we can load a predefined shape structure that is used for the segmentation method.

In Fig. 1 a predefined prior is used for segmenting finger bones and compare the segmentation result with a simple intensity thresholding and a segmentation with the pure GAC-energy. The result shows an identical segmentation result for the shape prior segmentation and the reference data labeled by an expert. A more difficult example is shown in Fig. 4 which shows a segmentation of a single vertebra in an X-ray image of the spline. Due to the very bad contrast simple thresholding would obviously fail completely and also pure GAC energy would end up into setting very much seed information.

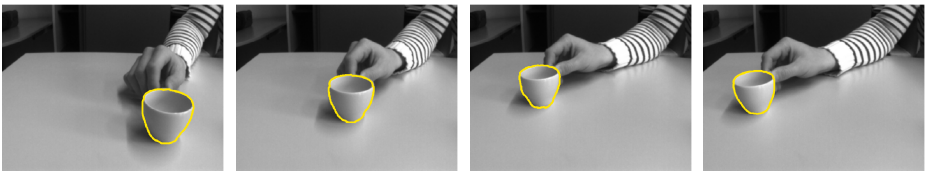

Fig. 7. Real-time tracking of an espresso cup in a live camera stream

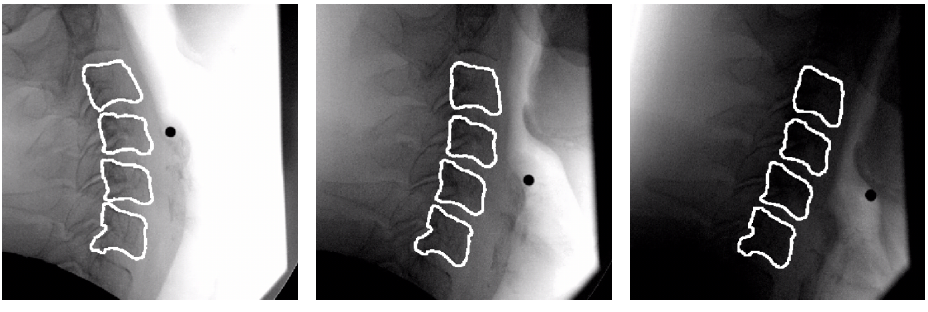

Fig. 8. Multiple vertebrae of the cervical spline are tracked separately through a sequence. The intention is to ascertain the movement of the vertebrae towards each other.

Fig. 9. Segmentation of bottles with a single shape prior

Examples of automated shape alignment with optimizing the transformation parameters in a local neighborhood are shown in Fig. 5–8. Fig. 5 shows again the labeled bone dataset. The overlay with reference data shows that the position optimization leads to the correct segmentation. For non-medical image data examples are presented in Fig. 6 and 7. The first one shows that the proposed method is robust against partial occlusion. Furthermore the method can be used

for tracking a certain structure over a sequence of frames. Fig. 7 shows a sequence of an espresso cup which was directly processed from a camera image with on-the-fly segmentation and position optimization. For a restricted domain of movement we gain real-time performance for tracking a sequence.

In Fig. 8 we track parts of the cervical spline in a moving X-ray image series to obtain a path of movement of the vertebrae to each other during a flexion. The predefined shapes of the four vertebrae are initialized in the first frame and than automatically tracked over the complete flexion. This can be used to ascertain shapes of implants for intervertebral discs.

In Fig. 9 multiple objects are segmented with the help of a single shape prior. Therefore a prior is defined in form of a bottle and placed roughly on each bottle in the image. The fine adjustments are done automatically.

5 Conclusion

In this paper, we proposed a globally optimal shape prior segmentation method with additional user interaction and automated position refinement. With this approach we can handle very different images and gain robust segmentation results. Especially the segmentation for difficult data like the low-contrast spline image benefits from the additional shape information. A great advantage of variational methods like this are the parallelization capability that especially profits by the modern graphics hardware that are able to boost the performance of such highly parallel algorithms.

References

1. Cremers, D., Tischhäuser, F., Weickert, J., Schnörr, C.: Diffusion snakes: Introducing statistical shape knowledge into the Mumford–Shah functional. International Journal of Computer Vision 50(3), 295–313 (2002)
2. Leventon, M., Faugeraus, O., Grimson, W.: Level set based segmentation with intensity and curvature priors. In: Workshop on Mathematical Methods in Biomedical Image Analysis, pp. 4–11 (2000)
3. Leventon, M., Grimson, W., Faugeras, O.: Statistical shape influence in geodesic active contours. In: Proc. IEEE Conference on Computer Vision and Pattern Recognition, vol. 1, pp. 316–323. IEEE, Los Alamitos (2000)
4. Paragios, N., Rousson, M., Ramesh, V.: Matching distance functions: A shape-to-area variational approach for global-to-local registration. In: Heyden, A., Sparr, G., Nielsen, M., Johansen, P. (eds.) ECCV 2002. LNCS, vol. 2351, pp. 775–789. Springer, Heidelberg (2002)
5. Paragios, N., Rousson, M., Ramesh, V.: Non-rigid registration using distance functions. Computer Vision and Image Understanding 89(2-3), 142–165 (2003)
6. Unger, M., Pock, T., Bischof, H.: Continuous Globally Optimal Image Segmentation with Local Constraints. In: Computer Vision Winter Workshop (2008)
7. Unger, M., Pock, T., Trobin, W., Cremers, D., Bischof, H.: TVSeg - Interactive total variation based image segmentation. In: British Machine Vision Conference (2008)

8. Mumford, D., Shah, J.: Optimal approximations by piecewise smooth functions and variational problems. Comm. on Pure and Applied Math. XLII(5), 577–685 (1988)
9. Chan, T.F., Vese, L.A.: Active contours without edges. IEEE Trans. Image Processing 10(2), 266–277 (2001)
10. Potts, R.B.: Some generalized order-disorder transformations. Proc. Camb. Phil. Soc. 48, 106–109 (1952)
11. Chan, T.F., Esedoglu, S., Nikolova, M.: Algorithms for finding global minimizers of image segmentation and denoising models. SIAM Journal of Applied Mathematics 66(5), 1632–1648 (2006)
12. Kass, M.: Snakes: Active contour models. International Journal of Computer Vision 1(4), 321–331 (1980)
13. Caselles, V., Kimmel, R., Sapiro, G.: Geodesic active contours. International Journal of Computer Vision 22(1), 61–79 (1997)
14. Kichenassamy, S., Kumar, A., Olver, P., Tannenbaum, A., Yezzi, A.: Conformal curvature flows: From phase transitions to active vision. Archive for Rational Mechanics and Analysis, 275–301 (1996)
15. Kichenassamy, S., Kumar, A., Olver, P.J., Tannenbaum, A.R., Yezzi Jr., A.J.: Gradient flows and geometric active contour models. In: International Conference on Computer Vision, pp. 810–815 (1995)
16. Leung, S., Osher, S.: Global minimization of the active contour model with TV-inpainting and two-phase denoising. In: Paragios, N., Faugeras, O., Chan, T., Schnörr, C. (eds.) VLSM 2005. LNCS, vol. 3752, pp. 149–160. Springer, Heidelberg (2005)
17. Bresson, X., Esedoglu, S., Vandergheynst, P., Thiran, J.P., Osher, S.J.: Global minimizers of the active contour/snake model. In: International Conference on Free Boundary Problems: Theory and Applications (FBP) (2005)
18. Bresson, X., Esedoglu, S., Vandergheynst, P., Thiran, J.P., Osher, S.J.: Fast global minimization of the active contour/snake model. J. of Mathematical Imaging and Vision 28(2), 151–167 (2007)
19. Chan, T.F., Esedoglu, S.: Aspects of total variation regularized L^1 function approximation. SIAM Journal of Applied Mathematics 65(5), 1817–1837 (2005)
20. Cremers, D., Schmidt, F.R., Barthel, F.: Shape priors in variational image segmentation: Convexity, Lipschitz continuity and globally optimal solutions. In: Computer Vision and Pattern Recognition, pp. 1–6 (2008)
21. Chan, T.F., Golub, G.H., Mulet, P.: A nonlinear primal-dual method for total variation-based image restoration. SIAM Journal on Scientific Computing 20(6), 1964–1977 (1999)
22. Carter, J.: Dual Methods for Total Variation-based Image Restoration. PhD thesis, UCLA (2001)
23. Chambolle, A.: An algorithm for total variation minimization and applications. Journal of Mathematical Imaging and Vision 20(1-2), 89–97 (2004)
24. Chambolle, A.: Total variation minimization and a class of binary MRF models. In: Rangarajan, A., Vemuri, B.C., Yuille, A.L. (eds.) EMMCVPR 2005. LNCS, vol. 3757, pp. 136–152. Springer, Heidelberg (2005)
25. Rudin, L.I., Osher, S.J., Fatemi, E.: Nonlinear total variation based noise removal algorithms. Physica D: Nonlinear Phenomena 60, 259–268 (1992)
26. Zhu, M., Chan, T.: An efficient primal-dual hybrid gradient algorithm for total variation image restoration. UCLA CAM Report 08-34 (2008)
27. Zhu, M., Wright, S.J., Chan, T.F.: Duality-based algorithms for total variation image restoration. UCLA CAM Report 08-33 (2008)